Published in final edited form as:

Bone. 2016 July ; 88: 138–145. doi:10.1016/j.bone.2016.04.028.

Postnatal β-catenin deletion from Dmp1-expressing osteocytes/osteoblasts reduces structural adaptation to loading, but not periosteal load-induced bone formation

Kyung Shin Kang[1], **Jung Min Hong**[1], and **Alexander G. Robling**[1,2,3,*]

[1]Department of Anatomy & Cell Biology, Indiana University School of Medicine, Indianapolis, IN, USA

[2]Department of Biomedical Engineering, Indiana University–Purdue University at Indianapolis, Indianapolis, IN, USA

[3]Richard L. Roudebush VA Medical Center, Indianapolis, IN, USA

Abstract

Mechanical signal transduction in bone tissue begins with load-induced activation of several cellular pathways in the osteocyte population. A key pathway that participates in mechanotransduction is Wnt/Lrp5 signaling. A putative downstream mediator of activated Lrp5 is the nucleocytoplasmic shuttling protein β-catenin (βcat), which migrates to the nucleus where it functions as a transcriptional co-activator. We investigated whether osteocytic βcat participates in Wnt/Lrp5-mediated mechanotransduction by conducting ulnar loading experiments in mice with or without chemically induced βcat deletion in osteocytes. Mice harboring βcat floxed loss-of-function alleles ($\beta cat^{f/f}$) were bred to the inducible osteocyte Cre transgenic ^{10kb}Dmp1-CreERt2. Adult male mice were induced to recombine the βcat alleles using tamoxifen, and intermittent ulnar loading sessions were applied over the following week. Although adult-onset deletion of βcat from Dmp1-expressing cells reduced skeletal mass, the bone tissue was responsive to mechanical stimulation as indicated by increased relative periosteal bone formation rates in recombined mice. However, load-induced improvements in cross sectional geometric properties were compromised in recombined mice. The collective results indicate that the osteoanabolic response to loading can occur on the periosteal surface when β-cat levels are significantly reduced in Dmp1-expressing cells, suggesting that either (i) only low levels of β-cat are required for mechanically induced bone formation on the periosteal surface, or (ii) other additional downstream mediators of Lrp5 might participate in transducing load-induced Wnt signaling.

[*]Corresponding Author: Alexander G. Robling, Ph.D., Department of Anatomy & Cell Biology, Indiana University School of Medicine, 635 Barnhill Dr., MS 5035, Indianapolis, IN 46202, Tel: (317) 274-7489, Fax: (317) 278-2040, arobling@iupui.edu.

Disclosure Statement: The authors have nothing to disclose.

Keywords

loading; mechanical strain; Wnt; β-catenin; osteoporosis

INTRODUCTION

Among the environmental factors that influence skeletal size and strength, mechanical loading is critical [1, 2]. Loss of adequate mechanical stimulation to bone tissue, as occurs in long-term bedrest, muscular paralysis, immobilization, and reduced gravitational environments, results in reduced bone mass and strength due to increased bone resorption and suppressed bone formation [3]. Conversely, enhanced mechanical stimulation to the skeleton has bone-building and/or anti-resorptive effects [4, 5]. Although the identity of the bone cell "mechanoreceptor" molecule(s)—which serves to monitor the mechanical environment surrounding the cell and generate a biochemical cascade inside the cell—is currently unresolved, it is becoming clear that the osteocyte is the cell type that receives and transduces mechanical information in bone [6, 7].

The molecular biology of osteocyte mechanotransduction is an unresolved field, but several key signaling pathways have been identified that have withstood the tests of time and experimental reproducibility. Among them is the Wnt pathway, which mediates many developmental and regulatory processes in numerous tissues [8, 9]. The importance of Wnt signaling in bone metabolism has been demonstrated in many clinical contexts; for example, the high-bone-mass (HBM) phenotypes in patients with activating mutations in the Wnt co-receptors Lrp5 [10] and Lrp4 [11], the HBM phenotypes in patients with inactivating mutations in the Lrp5/6 inhibitor Sost [12], and the low bone mass phenotypes in patients with inactivating mutations in Lrp5 [13] and Lrp6 [14].

Beyond its role in general bone metabolism, the Wnt pathway is intimately involved in bone cell mechanotransduction. Mechanical stimulation of cultured bone cells activates components of the canonical Wnt signaling cascade [15–18]. Moreover, genetic deletion of the Wnt co-receptor Lrp5, or overexpression of the Lrp5 inhibitor Sost, abolishes load-induced bone formation [19–22]. Conversely, activating mutations in Lrp5 enhance load-induced bone gain [21, 23]. While ample experimental evidence has defined Lrp5's role in mechanotransduction, the downstream mediators of mechanically activated Lrp5 are less well studied. Lrp5 is commonly thought to signal through the canonical Wnt pathway, which relies on the nucleocytoplasmic shuttling protein β-catenin (βcat) to promote Wnt-induced gene transcription [24, 25].

Although the skeletal phenotype of mice with βcat-deficient osteoblasts/osteocytes is superficially similar to that of mice with Lrp5-deficient osteoblasts/osteocytes (low bone mass phenotype), the cellular mechanisms driving their phenotypes are distinct. βcat-deficient mice exhibit low bone mass because of increased bone resorption with little to no changes in bone formation [26, 27], whereas Lrp5-deficient mice exhibit low bone mass because of reduced bone formation with little to no changes in bone resorption [20, 28]. Given that (1) mechanical loading stimulates bone formation through Lrp5, that (2) βcat is a key downstream signaling relay in the canonical Wnt/Lrp5 pathway, but (3) βcat plays a

prominent role in controlling bone resorption but not formation, it seems plausible that βcat might not be required for load-induced bone formation.

To assess the role of βcat in load-induced bone formation, we conducted *in vivo* mechanical loading studies using mice that harbored floxed loss-of-function βcat alleles ($\beta cat^{f/f}$) and a transgene for inducible Cre expression in osteocytes and late-stage osteoblasts (^{10kb}Dmp1-CreERt2) [29]. This approach permitted us to raise up phenotypically normal mice to adulthood, then induce deletion of βcat (via tamoxifen injection) from bone cells and immediately begin mechanical loading experiments. Our results indicate that although adult onset deletion of βcat from Dmp1-expressing cells reduced bone mass and density, osteocyte-selective inactivation of βcat did not prevent load-induced bone formation. However, geometric adaptation to loading was impaired. These findings indicate that the osteogenic response to loading can occur even with a deficiency of osteocytic β-cat, suggesting that other downstream mediators of Lrp5 might participate in transducing load-induced Wnt signaling.

MATERIALS AND METHODS

Experimental Mice

All mice were homozygous for a floxed loss-of-function βcat ($\beta cat^{f/f}$) allele that has been described previously [30]. Briefly, these mice harbor loxP sites in introns 1 and 6 of the βcat (*Ctnnb1*) gene. ^{10kb}Dmp1-CreERt2 transgenic mice have been described previously [29]. These mice harbor a cDNA for the Cre recombinase–mutant estrogen receptor fusion protein that results in Cre sequestration in the cytosol (away from the chromatin) until the selective ligand tamoxifen is encountered [31]. The CreERt2 gene was driven by a 10kb fragment of the Dentin Matrix Protein-1 (Dmp1) promoter, which provides osteocyte and late osteoblast selectivity of expression [32]. $\beta cat^{f/f}$ mice were maintained on a C57BL/6 background and ^{10kb}Dmp1-CreERt2 mice were maintained on a mixed 129/C57BL6 background. $\beta cat^{f/f}$ mice were bred to ^{10kb}Dmp1-CreERt2 over several generations to generate littermate $\beta cat^{f/f}$ mice that were either hemizygous (CreERt2+) for the ^{10kb}Dmp1-CreERt2 transgene or nontransgenic (CreERt2−) for the ^{10kb}Dmp1-CreERt2 transgene. Male mice were selected for the experiments. Offspring were same sex–housed in cages of three to five (independent of Cre genotype) and given standard mouse chow [Harlan Teklad 2018SX; 1% Ca; 0.65% P; vitamin D3 (2.1 IU/g)] and water ad libitum. All animal procedures were performed in accordance with relevant federal guidelines and conformed to the Guide for the Care and use of Laboratory Animals (8th Edition). The animal facility at Indiana University is an AAALAC-accredited facility.

Cre induction

To induce adult-onset recombination of the floxed βcat alleles, mice were treated with 20 mg/kg tamoxifen free base (M&P Biomedicals, Santa Ana, CA). Tamoxifen powder was dissolved in dimethyl formamide (DMF) at a concentration of 100mg/mL and then suspended in ~150 μL of corn oil for IP injection. Mice that received vehicle treatment (no Cre induction) were injected with an equivalent volume of DMF alone suspended in 150 μL of corn oil. Mice were treated with single injections of tamoxifen or vehicle 6 days prior and

3 days prior to the first day of loading, and again 3 days and 9 days after the first day of loading (4 total injections over the experiment). Details for the experimental schedule are shown in the Fig 1A. Visual monitoring of tissue specificity for Cre induction was qualitatively assessed by examining tissue sections from tamoxifen-treated Dmp1-CreErt2 transgenic mice that co-expressed the tdTomato (Ai9) Cre-reporter allele, which harbor a ubiquitously expressed flox-stop-flox-tdTomato cassette described elsewhere [32].

In vivo ulnar loading and fluorochrome labeling

Mice were loaded based on the ulna loading protocol originally described by Torrance et al [33]. At 18 weeks of age, 16 male mice of each Cre genotype began the ulnar loading regimen. A haversine waveform was used to apply load to the forelimb using a customized electromagnetic actuator at peak force of 2.85 N, 2 Hz, for 180 cycles/day. Before the in vivo loading sessions began, five additional mice from each group were sacrificed and the right forearm was fitted with a single element strain gauge (EA-06–015DJ-120; Measurements Group, Raleigh, NC, USA). The output from the strain gauge was measured on a digital oscilloscope as described previously [34]. For in vivo loading, each mouse was loaded once per day, every other day for a total of 3 loading days, beginning 3 days after the second tamoxifen injection. Calcein (12 mg/kg IP) and alizarin complexone (20 mg/kg IP) were injected 3 and 10 days, respectively, after the last loading bout. Mice were sacrificed 10 days after the alizarin injection. At sacrifice, the left (unloaded) and right (loaded) ulnae were dissected, cleaned and fixed in 10% NBF for 2 days followed by storage in 70% ethanol at 4°C.

Quantitative histomorphometry and geometric properties

The fixed ulnas were dehydrated in graded ethanols, cleared in xylene, and embedded in methylmethacrylate. Thick sections were collected at 1 to 1.5 mm distal to the midshaft (hereafter referred to as the “midshaft” location) using a diamond-embedded wafering saw. A second set of sections was collected 3 distal to midshaft (hereafter referred to as the “distal” location). Sections were ground and polished to ~30 μm, mounted and coverslipped, then digitally imaged on a fluorescent microscope. Periosteal and endocortical bone formation parameters were calculated at the midshaft and distal locations by measuring the extent of unlabeled perimeter (nL.Pm), single-labeled perimeter (sL.Pm), double-labeled perimeter (dL.Pm), and the area between the double labeling with Image-Pro software (MediaCybernetics Inc., Gaithersburg, MD). The derived histomorphometric parameters mineralizing surface (MS/BS), mineral apposition rate (MAR), and bone formation rate (BFR/BS) were calculated using standard procedures described elsewhere [35]. Relative load-induced bone formation parameters were calculated by subtracting the control arm value from the loaded arm value for each mouse.

Additionally, second moment of inertia (mm^4) was obtained from the digitized fluorescent midshaft ulnar images using the Moment macro in ImageJ software (NIH, Bethesda, MD). Each right (loaded) ulnar cross section used for fluorochrome histomorphometry was imported into ImageJ, in which the minimum second moments of area (I_{MIN}; mm^4) were calculated. The same parameters were calculated on the same sections a second time, but instead of using the bone surfaces as the section edge, the first label (which reveals the

relative position of the bone surface at the start of the experiment) was used to define the section. In regions of the periosteal perimeter where no labeling was detected, the final bone surface was used as the section edge. This allowed us to compare the initial bone area and geometry at the start of the experiment with the area and geometry at sacrifice in the same section, after the mechanical loading treatment had incurred its effects.

Dual-energy x-ray absorptiometry (DEXA)

Whole body DEXA scans were collected on isoflurane-anesthetized mice using a PIXImus II (GE Lunar) densitometer. All mice were scanned at 21 weeks of age, 2 days prior to sacrifice. From the whole body scans, areal bone mineral density (aBMD) and bone mineral content (BMC) were calculated for the entire postcranial skeleton and regionally for the lumbar spine (L3–L5, inclusive) and hindlimb (all skeletal tissue distal to the acetabulum) using the ROI tools. The spine and hindlimb subregion measurements served as a control to provide an indication of the effects of tamoxifen and of βcat deletion on general skeletal properties.

Laser capture microdissection and quantitative polymerase chain reaction (qPCR)

To assess whether βcat was selectively deleted in bone tissue and not in off-target tissues, we evaluated Dmp1 expression in both bone and muscle (positive control). Both CreERt2+ and CreERt2− mice were treated with either tamoxifen or oil as described above. Three days later, the mice were sacrificed and the right femur, including surrounding muscles, was removed, embedded in OCT, and immediately frozen by submersion in dry-ice-cooled isopentane. The blocks were mounted on the chuck of a cryostat, and 8 μm-thick sections were removed using a previously described tape-transfer system [36]. The sections were quickly dehydrated in 100% ethanol, air dried, and mounted to a custom slide compatible with a Leica LMD6500 laser capture microscope. Regions of cortical bone and skeletal muscle were individually collected into 0.5 ml caps using a 10X lens. Laser capture took less than 20 min per sample. RNAs were isolated using NucleoSpin RNA XS (Macherey-Nagel, Duren, Germany) following the manufacturer's instructions. Individual RNAs of each sample were used to make cDNAs using High Capacity cDNA Reverse Transcription Kits (Applied Biosystems) and these cDNAs were subjected to real-time PCR (Applied Biosystems 7900HT real-time PCR system). βcat (*Ctnnb1)* expression was quantitated using the $2^{-\Delta Ct}$ method and normalized to transcripts for the housekeeper GAPDH.

Statistical methods

Statistical analyses were computed using ANOVA, with Cre genotype (CreERt2+ or CreERt2−) and induction (tamoxifen or DMF) as main effects. Significance was taken at $P < 0.05$. Two-tailed distributions were used for all analyses and those data are presented as means ±SEM.

RESULTS

The induced Dmp1-CreERt2 transgene acts on floxed βcat alleles in bone but not muscle

To determine whether the mouse model we generated could reliably delete βcat in osteocytes, and simultaneously avoid recombination in other tissues, we treated CreERt2+

and CreERt2− mice with tamoxifen or oil, sacrificed them 3 days later, then measured βcat expression in isolated cortical bone tissue (target tissue) and skeletal muscle (control tissue) collected using laser capture microdissection (Fig 1C–D). Control experiments conducted in CreERt2− mice revealed that tamoxifen alone (*i.e.*, no Cre present to recombine floxed βcat alleles) reduced βcat expression in bone by 33% (Fig. 1C). Among CreERt2+ mice, tamoxifen reduced βcat in bone by 65% compared to oil-treated CreERt2+ mice, and by 72% compared to tamoxifen-treated CreERt2− mice. A similar effect of tamoxifen alone in CreERt2− mice was found in skeletal muscle samples (Fig 1D), but tamoxifen did not reduce muscle-specific βcat expression in CreERt2+ mice. tdTomato Cre-reporter mice revealed tamoxifen-induced recombination in osteocytes and some surface cells, but not in muscle (Fig. S1).

Adult onset deletion of βcat from Dmp1-expressing cells reduces skeletal mass and density

As an additional control experiment, we probed for changes in spine, lower limb, and total body bone mineral density and content among CreERt2+ and CreERt2− mice treated with tamoxifen or oil. This analysis was undertaken to confirm that we were successfully deleting βcat from the skeleton of adult mice, as βcat deletion from bone previously has been shown to reduce skeletal mass and density [37]. In CreERt2− mice, tamoxifen had no significant effect on BMC or BMD compared to oil treatment, in any of the skeletal regions analyzed (whole body, spine, hindlimb; Fig 2). In CreERt2+ mice, tamoxifen treatment significantly reduced whole body and spinal BMD and BMC compared to oil treatment, but the tamoxifen-induced reduction observed for the hindlimb did not reach significance.

Deletion of βcat from Dmp1-expressing cells does not prevent load-induced periosteal bone formation, but endocortical bone formation and geometric adaptation are impaired

To determine whether βcat in osteocytes/late-stage osteoblasts is required for load-induced bone formation, we applied mechanical stimulation to the ulnae of CreERt2− and CreERt2+ mice treated with tamoxifen or oil before and during a 1-wk loading regimen. Before looking at load-induced bone formation, we first evaluated the effects of tamoxifen alone and βcat deletion on histomorphometric measurements in the control ulnae. In the nonloaded limbs of CreERt2− mice, tamoxifen treatment resulted in a significant increase in periosteal MAR and BFR/BS (Fig. 3A–C; Fig. S2), indicating mildly anabolic properties of tamoxifen alone that others have reported [38, 39]. Conversely, in the nonloaded limbs of CreERt2+ mice, tamoxifen treatment resulted in a significant decrease in periosteal MS/BS and BFR/BS, likely the result of βcat deletion. No differences in mechanical strain were detected among groups from the *ex vivo* strain gauging tests ($\dot{x}$ = 2740–2980 με ± 58–95με; ANOVA p=0.64). All four groups exhibited significant increases in periosteal MS/BS, MAR, and BFR/BS, in the loaded ulna compared to the nonloaded ulna (Fig. 3A–C). To compare the degree of load-induced bone formation parameters achieved among the different treatment/genotype groups, we normalized load-induced bone formation values (right ulna) to control limb bone formation values (left ulna) using a relative (right minus left) calculation approach (Fig. 3D–F). No deficiencies in relative MS/BS, MAR, or BFR/BS were found among the mice with βcat deletion, suggesting that anabolic mechanotransduction proceeded normally despite a significant reduction in osteocytic/late-osteoblastic βcat. On the endocortical

surface, tamoxifen stimulated a significant increase in BFR/BS in the nonloaded limb, regardless of Cre status (Fig S3). Load-induced endocortical bone formation rates were increased among oil-treated mice but not among tamoxifen-treated mice, regardless of Cre status (Fig. S3).

In order to assess changes in ulnar adaptation to loading via alterations in cross sectional geometric properties, we calculated the second moment of area along the minor axis (I_{MIN}) of each digitized histological before loading (preloading; indicated by the calcein label) and after loading (postloading; indicated by the bone edge). Loading significantly increased I_{MIN} in all four groups (Fig. 4), to a similar degree reported in previous experiments [34]. However, the ratio of postload to preload I_{MIN} was significantly lower in the tamoxifen-treated CreERt2+ group (βcat deletion) compared to the remaining three groups. Areal properties (Tt.Ar and B.Ar) flowed similar trends to those reported for geometric properties (Table S1). Those data suggest that while bone formation proceeded relatively normally in loaded mice that lacked βcat, the geometric and areal adaptation was not as robust as was observed in the βcat replete mice.

DISCUSSION

Our primary objective in this study was to understand whether osteocytic βcat regulates the osteogenic response to mechanical loading. Our results indicate that while βcat deletion from osteocytes reduced resting (nonloaded limb) bone formation, mechanical loading significantly increased periosteal bone formation despite a 65% reduction in βcat expression. For these experiments, we chose to use an inducible Cre model (^{10kb}Dmp1-CreERt2) to recombine the floxed βcat alleles ($\beta cat^{f/f}$) in adult mice for two reasons. First, $\beta cat^{f/f}$ mice that harbor the non-inducible ^{10kb}Dmp1-Cre transgene do not survive beyond 8–12 wks [37]. *In vivo* mechanotransduction studies are most informative when conducted after the growth phase is completed (17 wks of age), so our mouse model approach had the advantage of permitting experiments in skeletally mature animals. Second, we were able to conduct the loading experiments on mice that had a phenotypically normal skeleton. When mutations exert their effects on the skeleton from conception onward, the size, shape, structure, and material properties at skeletal maturity can be very different from wild type, non-mutant mice due to a lifelong accumulation of effects caused by the mutation. We were able to induce βcat deletion and immediately begin loading the ulna. This approach more accurately models a scenario of compromised cellular signaling, rather than a cumulative effect on tissue properties.

Although load-induced increase in relative (i.e., normalized to the nonloaded left arm) periosteal bone formation in mice with βcat deletion was statistically similar to the control groups, the absolute increase (i.e., not normalized to the nonloaded left arm) in periosteal BFR/BS in the loaded arm was reduced in induced mice. This outcome had the effect of generating a significant reduction in the load-induced change in the minimum second moment of area (I_{MIN}) among induced mice compared to the control groups, as the change from baseline in the loaded arm (rather than difference from nonloaded arm) was used to calculate load-induced changes in the second moment. It is also possible that the mutation produced poorer localization of new bone to the high-strain periosteal surfaces, which would

also affect the change in second moment of area. Other molecules in the Wnt pathway (e.g., Sost) are known to control the distribution of new bone formation as a function of mechanical strain, so it is possible that βcat might also participate in this effect [40]. Lastly, we observed a blunted response to loading on the endocortical surface among induced mice, which could have contributed to the lack of geometric adaptation in those samples.

Mechanical stimulation activates Wnt signaling in osteoblasts and osteocytes. Osteoblasts subjected to stretching or fluid shear stress exhibit many hallmarks of activated canonical Wnt, including translocation of βcat to the nucleus and Wnt target gene (or reporter gene) expression [16, 17]. We and others found that loss of Lrp5 either globally [20, 21], or locally in Dmp1-expressing cells [41], inhibits load-induced bone formation, which casts little doubt that Wnt/Lrp5 is required for mechanotransduction in bone. It is therefore perplexing that the putative key downstream node in activated Lrp5 signaling—βcat—in the same cell type (Dmp1-expressing) is dispensable for load-induced bone formation. Further evidence for a disconnect between Lrp5 and βcat has been reported recently, where load-induced βcat reporter expression *in vivo* can occur independent of Lrp5/6 activation [42].

Recently, Javaheri *et al.* reported that deletion of a single copy of βcat in osteocytes beginning at conception (^{10kb}Dmp1-Cre × βcat$^{+/f}$) abolished the anabolic response to mechanical loading in 18–24 wk-old mice [43]. While their loading protocol employed similar levels of strain (2500 με vs. our 2800 με) but a longer duration (3 wks vs. our 1 wk), their conclusions diverge from ours in some aspects. Several experimental design differences between the two studies are noteworthy and might explain the inconsistencies in results. First, we used a tamoxifen-inducible Cre model in homozygous floxed mice, whereas their experiments were conducted using a stable Cre model in heterozygous floxed mice. At least one report indicates that tamoxifen can complicate mechanotransduction studies by enhancing load-induced bone formation [44]. We attempted to control for this effect by measuring the effect of corn oil or tamoxifen administration to CreERt2− mice (i.e., no CreErt2 target for tamoxifen) on the loading response. A significant tamoxifen-associated increase in periosteal bone formation rate was detected in the non-loaded ulna, but not in the loaded ulna. It is possible, however, that tamoxifen still had some influence on load-induced bone formation in the CreERt2+ mice (i.e., interaction with βcat loss) that was not detected by our design. Second, we used homozygous βcat flox mouse model rather than a heterozygous model. We measured an 80% reduction in βcat expression in tamoxifen-treated CreERt2+ mice, compared to oil-treated CreERt2− mice; it is unclear the degree of βcat suppression achieved by the ^{10kb}Dmp1-Cre × βcat$^{+/f}$ reported in [43] was greater or less than the level of suppression we generated. Third, unlike the ^{10kb}Dmp1-Cre transgenic, the ^{10kb}Dmp1-CreERt2 model avoids recombination in skeletal muscle if the transgene is induced postnatally. As considerable muscle–bone crosstalk axis has been identified in recent years, it is unclear whether βcat deletion from skeletal muscle influences mechanical signaling in bone via yet unidentified myokines [45].

This study has several inherent limitations. First, the Cre mouse model we chose to use for these experiments precluded the possibility of gene deletion without the confounding effects of tamoxifen. We attempted to address this limitation experimentally by including CreERt2− controls that were treated with and without tamoxifen. Second, our use of the inducible Cre

model, in contrast to the non-inducible Dmp1-Cre model, might have resulted in retention of a subpopulation of osteocytes that escaped recombination after tamoxifen induction. This is possible because the Dmp1 promoter is more active in early osteocytes and exhibits markedly reduced expression in mature osteocytes. Thus, some of the mature osteocytes might not have recombined one or both βcat alleles due to downregulated transgene promoter activity. If so, the "escaped" osteocytes might be capable of contributing to the load-induced bone formation we observed in otherwise recombined tissue. Lastly, the inducible Dmp1-CreERt2 model exhibits a measureable amount of "leakiness." We report here (e.g., Fig. 1) and others report elsewhere [32] that this mouse model undergoes recombination in a fraction of cells in the absence of tamoxifen. Previous reports using tdTomato fluorescent reporter mice indicated that 10–20% of the osteocytes undergo recombination prior to chemical induction [32], whereas our expression studies from laser captured cortical tissue indicate that the floxed βcat gene exhibited around 40% reduction in unprovoked recombination. It is likely that each gene will have different sensitivities to unprovoked recombination based on accessibility of the loxP sites and other local nuclear matrix properties.

In conclusion, our experiments suggest that osteocyte-selective βcat deletion from the adult skeleton leads to a decrease in skeletal mass and density, but not in periosteal load-induced bone formation at the ulnar midshaft. However, the preserved effects of mechanical stimulation in βcat-deficient mice were not observed on the endocortical surface and did not translate into improvements in the second moment of area, a hallmark of mechanical adaptation in nonmutant mice. These findings suggest that the role of βcat in mechanotransduction might be more complicated than previously thought, and raise the possibility that other additional downstream mediators (or effectors) of Wnt/Lrp5 might transduce mechanical signals in bone tissue.

Supplementary Material

Refer to Web version on PubMed Central for supplementary material.

Acknowledgments

Grant support:

This work was supported by NIH grants AR53237 and BX001478 (to AGR).

References

1. Robling AG, Castillo AB, Turner CH. Biomechanical and molecular regulation of bone remodeling. Annual review of biomedical engineering. 2006; 8:455–98.
2. Rubin CT, Lanyon LE. Regulation of bone mass by mechanical strain magnitude. Calcified tissue international. 1985; 37(4):411–7. [PubMed: 3930039]
3. Leblanc AD, et al. Bone mineral loss and recovery after 17 weeks of bed rest. Journal of bone and mineral research: the official journal of the American Society for Bone and Mineral Research. 1990; 5(8):843–50.
4. Jones HH, et al. Humeral hypertrophy in response to exercise. The Journal of bone and joint surgery American volume. 1977; 59(2):204–8. [PubMed: 845205]

5. Robling AG, et al. Improved bone structure and strength after long-term mechanical loading is greatest if loading is separated into short bouts. Journal of bone and mineral research: the official journal of the American Society for Bone and Mineral Research. 2002; 17(8):1545–54.
6. Burger EH, et al. Function of osteocytes in bone--their role in mechanotransduction. The Journal of nutrition. 1995; 125(7 Suppl):2020S–2023S. [PubMed: 7602386]
7. Mullender M, et al. Mechanotransduction of bone cells in vitro: mechanobiology of bone tissue. Medical & biological engineering & computing. 2004; 42(1):14–21. [PubMed: 14977218]
8. Bonewald LF. The amazing osteocyte. Journal of bone and mineral research: the official journal of the American Society for Bone and Mineral Research. 2011; 26(2):229–38.
9. Bonewald LF, Johnson ML. Osteocytes, mechanosensing and Wnt signaling. Bone. 2008; 42(4): 606–15. [PubMed: 18280232]
10. Little RD, et al. A mutation in the LDL receptor-related protein 5 gene results in the autosomal dominant high-bone-mass trait. American journal of human genetics. 2002; 70(1):11–9. [PubMed: 11741193]
11. Leupin O, et al. Bone overgrowth-associated mutations in the LRP4 gene impair sclerostin facilitator function. The Journal of biological chemistry. 2011; 286(22):19489–500. [PubMed: 21471202]
12. Balemans W, et al. Increased bone density in sclerosteosis is due to the deficiency of a novel secreted protein (SOST). Human molecular genetics. 2001; 10(5):537–43. [PubMed: 11181578]
13. Gong Y, et al. LDL receptor-related protein 5 (LRP5) affects bone accrual and eye development. Cell. 2001; 107(4):513–23. [PubMed: 11719191]
14. Mani A, et al. LRP6 mutation in a family with early coronary disease and metabolic risk factors. Science. 2007; 315(5816):1278–82. [PubMed: 17332414]
15. Armstrong VJ, et al. Wnt/beta-catenin signaling is a component of osteoblastic bone cell early responses to load-bearing and requires estrogen receptor alpha. The Journal of biological chemistry. 2007; 282(28):20715–27. [PubMed: 17491024]
16. Hens JR, et al. TOPGAL mice show that the canonical Wnt signaling pathway is active during bone development and growth and is activated by mechanical loading in vitro. Journal of bone and mineral research: the official journal of the American Society for Bone and Mineral Research. 2005; 20(7):1103–13.
17. Norvell SM, et al. Fluid shear stress induces beta-catenin signaling in osteoblasts. Calcified tissue international. 2004; 75(5):396–404. [PubMed: 15592796]
18. Robinson JA, et al. Wnt/beta-catenin signaling is a normal physiological response to mechanical loading in bone. The Journal of biological chemistry. 2006; 281(42):31720–8. [PubMed: 16908522]
19. Iwaniec UT, et al. PTH stimulates bone formation in mice deficient in Lrp5. Journal of bone and mineral research: the official journal of the American Society for Bone and Mineral Research. 2007; 22(3):394–402.
20. Sawakami K, et al. The Wnt co-receptor LRP5 is essential for skeletal mechanotransduction but not for the anabolic bone response to parathyroid hormone treatment. The Journal of biological chemistry. 2006; 281(33):23698–711. [PubMed: 16790443]
21. Saxon LK, et al. Analysis of multiple bone responses to graded strains above functional levels, and to disuse, in mice in vivo show that the human Lrp5 G171V High Bone Mass mutation increases the osteogenic response to loading but that lack of Lrp5 activity reduces it. Bone. 2011; 49(2):184–93. [PubMed: 21419885]
22. Tu X, et al. Sost downregulation and local Wnt signaling are required for the osteogenic response to mechanical loading. Bone. 2012; 50(1):209–17. [PubMed: 22075208]
23. Niziolek PJ, Warman ML, Robling AG. Mechanotransduction in bone tissue: The A214V and G171V mutations in Lrp5 enhance load-induced osteogenesis in a surface-selective manner. Bone. 2012; 51(3):459–65. [PubMed: 22750014]
24. Baron R, Rawadi G. Targeting the Wnt/beta-catenin pathway to regulate bone formation in the adult skeleton. Endocrinology. 2007; 148(6):2635–43. [PubMed: 17395698]
25. Moon RT, et al. WNT and beta-catenin signalling: diseases and therapies. Nature reviews Genetics. 2004; 5(9):691–701.

26. Yadav VK, et al. Lrp5 controls bone formation by inhibiting serotonin synthesis in the duodenum. Cell. 2008; 135(5):825–37. [PubMed: 19041748]
27. Chang MK, et al. Reversing LRP5-dependent osteoporosis and SOST deficiency-induced sclerosing bone disorders by altering WNT signaling activity. Journal of bone and mineral research: the official journal of the American Society for Bone and Mineral Research. 2014; 29(1): 29–42.
28. Kedlaya R, et al. Sclerostin Inhibition Reverses Skeletal Fragility in an Lrp5-Deficient Mouse Model of OPPG Syndrome. Sci Transl Med. 2013; 5(211)
29. Powell WF Jr, et al. Targeted ablation of the PTH/PTHrP receptor in osteocytes impairs bone structure and homeostatic calcemic responses. The Journal of endocrinology. 2011; 209(1):21–32. [PubMed: 21220409]
30. Brault V, et al. Inactivation of the beta-catenin gene by Wnt1-Cre-mediated deletion results in dramatic brain malformation and failure of craniofacial development. Development. 2001; 128(8): 1253–64. [PubMed: 11262227]
31. Indra AK, et al. Temporally-controlled site-specific mutagenesis in the basal layer of the epidermis: comparison of the recombinase activity of the tamoxifen-inducible Cre-ER(T) and Cre-ER(T2) recombinases. Nucleic acids research. 1999; 27(22):4324–7. [PubMed: 10536138]
32. Kalajzic I, et al. In vitro and in vivo approaches to study osteocyte biology. Bone. 2013; 54(2):296–306. [PubMed: 23072918]
33. Torrance AG, et al. Noninvasive loading of the rat ulna in vivo induces a strain-related modeling response uncomplicated by trauma or periostal pressure. Calcified tissue international. 1994; 54(3):241–7. [PubMed: 8055374]
34. Robling AG, et al. Evidence for a skeletal mechanosensitivity gene on mouse chromosome 4. FASEB journal: official publication of the Federation of American Societies for Experimental Biology. 2003; 17(2):324–6. [PubMed: 12490544]
35. Dempster DW, et al. Standardized nomenclature, symbols, and units for bone histomorphometry: a 2012 update of the report of the ASBMR Histomorphometry Nomenclature Committee. Journal of bone and mineral research: the official journal of the American Society for Bone and Mineral Research. 2013; 28(1):2–17.
36. Nakano Y, et al. Site-specific localization of two distinct phosphatases along the osteoblast plasma membrane: tissue non-specific alkaline phosphatase and plasma membrane calcium ATPase. Bone. 2004; 35(5):1077–85. [PubMed: 15542032]
37. Kramer I, et al. Osteocyte Wnt/beta-catenin signaling is required for normal bone homeostasis. Molecular and cellular biology. 2010; 30(12):3071–85. [PubMed: 20404086]
38. Perry MJ, et al. Tamoxifen stimulates cancellous bone formation in long bones of female mice. Endocrinology. 2005; 146(3):1060–5. [PubMed: 15576459]
39. Starnes LM, et al. Increased bone mass in male and female mice following tamoxifen administration. Genesis. 2007; 45(4):229–35. [PubMed: 17417806]
40. Robling AG, et al. Mechanical stimulation of bone in vivo reduces osteocyte expression of Sost/sclerostin. The Journal of biological chemistry. 2008; 283(9):5866–75. [PubMed: 18089564]
41. Zhao L, et al. Inactivation of Lrp5 in osteocytes reduces young's modulus and responsiveness to the mechanical loading. Bone. 2013; 54(1):35–43. [PubMed: 23356985]
42. Lara-Castillo N, et al. In vivo mechanical loading rapidly activates beta-catenin signaling in osteocytes through a prostaglandin mediated mechanism. Bone. 2015; 76:58–66. [PubMed: 25836764]
43. Javaheri B, et al. Deletion of a single beta-catenin allele in osteocytes abolishes the bone anabolic response to loading. Journal of bone and mineral research: the official journal of the American Society for Bone and Mineral Research. 2014; 29(3):705–15.
44. Sugiyama T, et al. Mechanical loading-related bone gain is enhanced by tamoxifen but unaffected by fulvestrant in female mice. Endocrinology. 2010; 151(12):5582–90. [PubMed: 20943807]
45. Bonewald LF, et al. Forum on bone and skeletal muscle interactions: summary of the proceedings of an ASBMR workshop. Journal of bone and mineral research: the official journal of the American Society for Bone and Mineral Research. 2013; 28(9):1857–65.

Highlights

- Adult-onset deletion of β-catenin from Dmp1-expressing cells results in measurable reduction in bone mass and density over a 4-wk period.
- Mice with induced deletion of β-catenin in Dmp1-expressing cells were responsive to mechanical stimulation, though baseline bone formation was suppressed
- Geometric adaptation of the midshaft ulna was compromised in loaded β-catenin deficient mice.

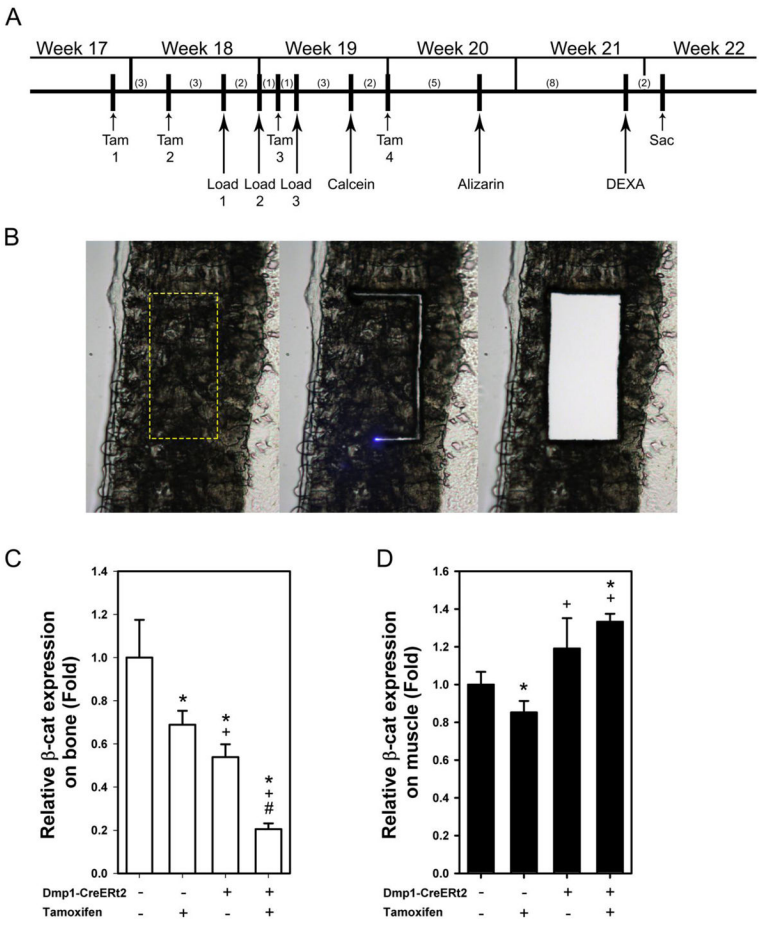

Fig. 1.

(A) Schematic diagram of the experimental design. To induce recombination of the floxed βcat alleles in fully adult mice, tamoxifen (Tam) was first injected at 17 wks of age, then several times thereafter to ensure recombination. Numbers in parentheses indicate days between manipulations. (B) To assess βcat expression in bone and muscle after tamoxifen-induced Cre translocation, RNA from cortical bone and muscle were collected by laser capturing technique from frozen sections. Moving from left to right, the panels show a portion of the femur cortex with the laser ROI indicated by the dashed box (left), the section midway through the laser capture process (middle), and the section after the defined cortical bone region had dropped into the cap (right) for analysis. Original lens magnification is 10X. (C) Real time PCR revealed a significant tamoxifen-induced reduction in βcat expression in the laser captured fragments in both Cre genotypes (* $p < 0.05$ compared to CreERt2− with Oil group, + $p < 0.05$ compared to CreERt2− with tamoxifen group, # $p < 0.05$ compared to CreERt2+ with Oil group) and a roughly 50% reduction in βcat expression among CreERt2+ mice that were not exposed to tamoxifen. (D) βcat expression in muscle fragments was fairly consistent across genotype/treatment (with the exception of tamoxifen-treated CreERt2− mice) groups, indicating a lack of Cre nuclear activity in muscle tissue with this model. Sample size is n=10/group.

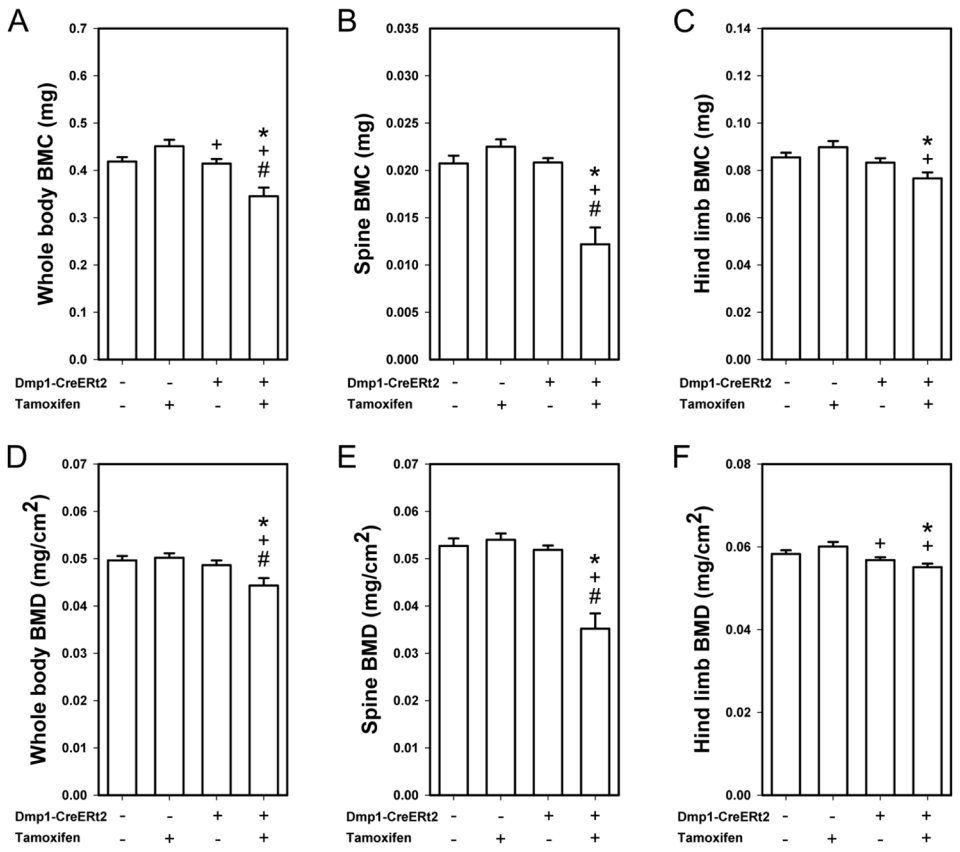

Fig. 2.

Bone mineral content (BMC) was measured by DEXA at the end of the experiment (21 wks of age) using an ROI that encompassed (A) the whole body, (B) the lumbar spine (L3–L5, inclusive), and (C) the hindlimb (all skeletal tissue distal to the acetabulum). Tamoxifen reduced BMC in Cre-positive mice but not in Cre negative mice (* $p < 0.05$ compared to CreERt2− with Oil group, + $p < 0.05$ compared to CreERt2− with tamoxifen group, # $p < 0.05$ compared to CreERt2+ with Oil group). (D–F) Bone mineral density (BMD) was also obtained from the same DEXA scans, and yielded similar reductions in skeletal properties among the βcat–recombined mice. Sample size is n=10/group.

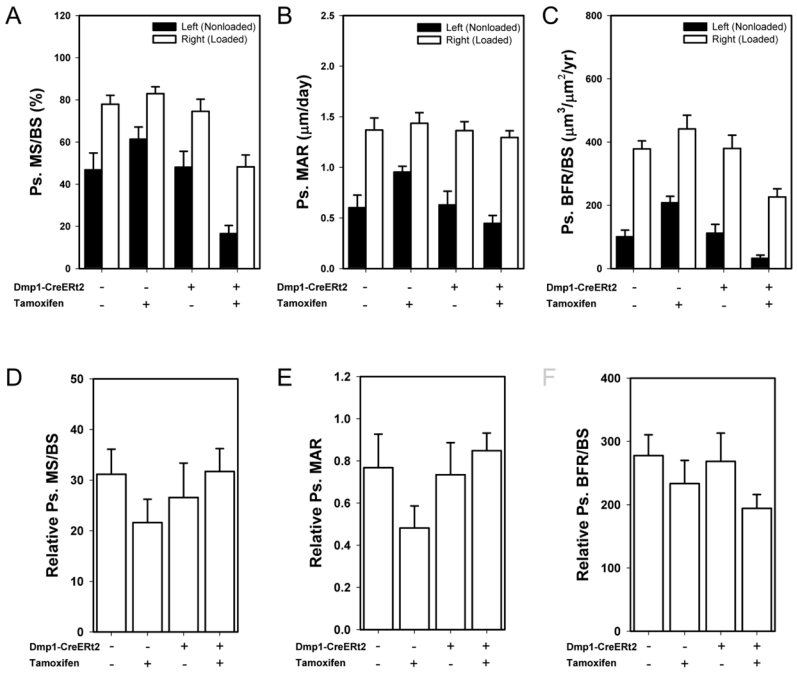

Fig. 3.

Mechanical loading generated new bone formation at the ulnar midshaft site in Cre-induced and control mice. (A) Periosteal mineralizing surface per bone surface (MS/BS; panel B), periosteal mineral apposition rate (MAR; panel C), and periosteal bone formation rate per unit bone surface (BFR/BS; panel D) were all significantly increased by mechanical loading, compared to the control ulna, within each genotype/treatment group (not indicated by symbols in figure; * $p < 0.05$ compared to CreERt2− with Oil group, + $p < 0.05$ compared to CreERt2− with tamoxifen group, # $p < 0.05$ compared to CreERt2+ with Oil group). (E–G) Relative values (right minus left) were calculated for each dynamic formation parameter to adjust loading effects for genotype/treatment changes in the baseline (revealed by the nonloaded ulna) parameters. The anabolic effect of mechanical loading was not significantly inhibited by βcat deletion in tamoxifen-treated CreERt2+ group compared to the remaining three groups. Sample size is n=10/group.

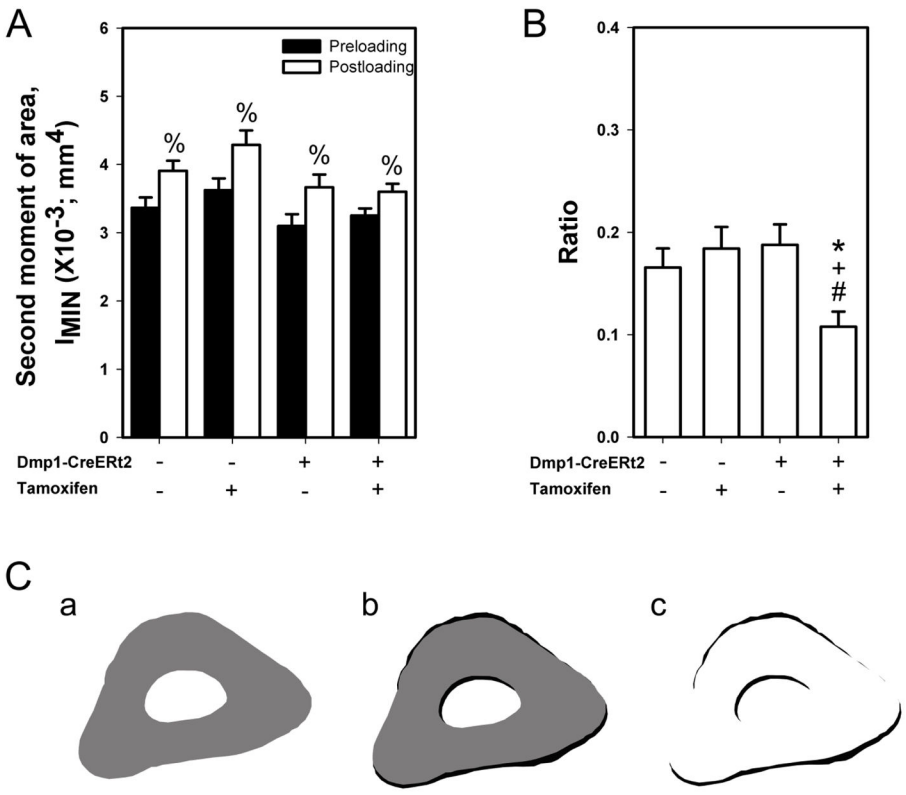

Fig. 4.

Cross-sectional moments of inertia were calculated from the loaded ulnar sections to quantify changes in ulnar adaptation to mechanical loading. (A) Second moment of area along the minor axis (I_{MIN}) was calculated before loading (preloading; indicated by the calcein label) and after loading (postloading; indicated by the bone edge). % indicates $p < 0.05$ compared to preloading values. (B) The ratio of postloading to preloading second moment was significantly lower in the βcat recombined group compared to the remaining three groups (* $p < 0.05$ compared to CreERt2− with Oil group, + $p < 0.05$ compared to CreERt2− with tamoxifen group, # $p < 0.05$ compared to CreERt2+ with Oil group). (C) Representative ulnar images of (a) preloading (grey), (b) postloading (black), and (c) areal difference between preloading and postloading (black), showing typical geometric adaptation in a control mouse. Sample size for the second moment of area is n=10/group.